Journal of Applied Polymer Science

Dynamic mechanical and shape memory properties of polybenzoxazines based on aminopropyl-terminated siloxanes

Xuehui Su, Shuning Song, Chunhui Zhang, Jinbai Huang, Yanfang Liu, Mingtao Run, Yonggang Wu
Key Laboratory of Analytical Science and Technology of Hebei Province College of Chemistry and Environmental Science, Hebei University, Baoding 071002, China
Correspondence to: Y. Liu (E-mail: liuyanfang@msn.com)

ABSTRACT: Four siloxane-containing benzoxazine monomers and telechelic benzoxazine oligomers were synthesized from 1,3-bis(3-aminopropyl)-1,1,3,3-tetramethyldisiloxane, α,ω-bis(3-aminopropyl)polydimethylsiloxane, phenol, *o*-allylphenol, and formaldehyde. The length of the siloxane segment affects the polymerization reaction of the benzoxazine monomers and telechelic benzoxazine oligomers. The dynamic mechanical properties of the corresponding polybenzoxazines depend primarily on the structure of phenol and the length of the siloxane segment. The polybenzoxazines exhibit one-way dual-shape memory behavior in response to changes in temperature. The thermally induced shape memory effects of the polybenzoxazines were characterized by bending and tensile stress–strain tests with a temperature program based on their glass transition temperatures. © 2016 Wiley Periodicals, Inc. J. Appl. Polym. Sci. **2016**, *133*, 44121.

KEYWORDS: properties and characterization; resins; ring-opening polymerization; stimuli-sensitive polymers; thermosets

Received 10 February 2016; accepted 23 June 2016
DOI: 10.1002/app.44121

INTRODUCTION

Shape memory polymers (SMPs) are a class of stimuli-responsive materials which have the ability to be deformed and fixed in a temporary shape and then recovered to their original shape induced by an appropriate external stimulus, such as heat, light, humidity, solvent, pH, and electric or magnetic fields.[1–6] In the past decade, SMPs have attracted much attention from academic and industrial researchers due to their promising applications in biomedicine, packaging, textile, construction, electronics, and aerospace.[7–12]

In general, SMPs require a suitable polymer network architecture consisting of netpoints and switch segments.[1–6] The netpoints can be of either physical or chemical nature, which define the permanent shape of SMPs. The molecular switches are comprised of stimuli-sensitive chain segments, which provide additional temporary crosslinks that stabilize the temporary shape. For SMPs, the netpoints and switch segments play key roles in determining the shape memory performance.

The commonly used approaches to preparing shape memory polymers are based on using either physical or chemical crosslinks to construct the required network structure. Benzoxazines are a class of heterocyclic compounds that can be polymerized into polybenzoxazines with a crosslinked network structure. From an SMP structural point of view, the crosslinked network can endow polybenzoxazines with a shape memory effect (SME). Over the past three years, some reports have been published on the use of crosslinked networks of polybenzoxazine as a second set of netpoints to support a permanent shape.[13–16] Recently, two research articles were reported on SME for neat polybenzoxazines.[17,18] Depending on the considerable molecule design flexibility, benzoxazines with different structures can be synthesized by changing the starting materials to tune the relationship between structure and properties, and the resultant polybenzoxazines would exhibit SMEs.

In practice, many researchers incorporate flexible —Si—O—Si— linkages into benzoxazine molecules to improve the processability and brittleness of polybenzoxazines,[19–29] and various siloxane-containing benzoxazines were synthesized from 1,3-bis(3-aminopropyl)tetramethyldisiloxane,[19] 3-aminopropyltriethoxysilane,[20] α,ω-bis(aminopropyl)polydimethylsiloxane,[21–23] siloxane-containing dihydroxyl compounds,[24,25] and γ-aminopropyldimethoxy-methylsilane and dimethyldiethoxysilane,[26] or from hydrosilylation reaction of allyl-containing benzoxazines with 1,1,3,3-tetramethyldisiloxane and hydride terminated polydimethylsiloxane.[27–29] These works incorporated different siloxanes into benzoxazines, which enhance the properties of the resultant polybenzoxazines, such as glass transition temperature (T_g) and toughness,[19,22,26] thermal stability,[20,22–25,27–29] flame retardancy,[20] surface hydrophobicity,[21] elongation at break,[22,26]

Additional Supporting Information may be found in the online version of this article.

and flexibility,[29] but they did not involve the research on SME for polybenzoxazines.

In this article we report the synthesis, polymerization behavior, dynamic mechanical properties, and shape memory properties of siloxane-containing benzoxazine monomers and telechelic benzoxazine oligomers,[30,31] starting from 1,3-bis(3-aminopropyl)-1,1,3,3-tetramethyldisiloxane (APTMDS), α,ω-bis(3-aminopropyl)polydimethylsiloxane (APPDMS), phenol, *o*-allylphenol, and formaldehyde. Structure variations were made in order to study the influence of siloxane segment length and phenolic structure on the polymerization behavior of benzoxazine monomers and telechelic benzoxazine oligomers and dynamic mechanical and shape memory properties of the resultant polybenzoxazines. In this respect, the polymerization temperatures, storage moduli, glass transition temperatures, and shape memory performance were taken into account.

EXPERIMENTAL

Materials

APTMDS (molecular weight $M = 248.51$ g/mol) was purchased from Shanghai Chuqing Organosilane Technology Co., Ltd., China. APPDMS (number-average molecular weight $M_n \approx 1070$ g/mol) was purchased from Hangzhou Silong Material Technology Co., Ltd., China. Phenol, formaldehyde (37% aqueous), toluene, and chloroform were obtained from Tianjin Chemical Reagent Co., Ltd., China. *o*-Allylphenol was supplied by Shandong Laizhou Hualu Storage Battery Co., Ltd., China. All chemicals were used as received.

Synthesis of Siloxane-Containing Benzoxazine Monomers and Telechelic Benzoxazine Oligomers

1,3-Bis(3-(2H-benzo[e][1,3]oxazin-3(4H)-yl)propyl)-1,1,3,3-tetramethyldisiloxane (P-APTMDS). In a 250 mL three-necked round bottom flask equipped with a mechanical stirrer, a thermometer, and a reflux condenser, 20 mL of formaldehyde and 20 mL of toluene were added. Then, the mixture was stirred in an ice bath and 15.7 g of APTMDS in 20 mL of toluene was added with a pressure-equalizing dropping funnel. After 11.5 mL of phenol was added, the temperature was raised gradually up to 86 °C and kept stirring for 24 h. Thereafter, the solvent was removed by distillation under reduced pressure, and the residue was dissolved in 20 mL of chloroform, followed by washing with 1 mol/L NaOH aqueous solution, 0.1 mol/L HCl aqueous solution, and deionized water for several times, respectively. After the chloroform was evaporated under reduced pressure, the product was dried at 40 °C in a vacuum oven for 24 h. Finally a pale-yellow, transparent, viscous liquid was obtained, and the yield was approximately 75%.

α,ω-Bis((3-(2H-benzo[e][1,3]oxazin-3(4H)-yl)propyl) polydimethylsiloxane (P-APPDMS). P-appdms was synthesized by a procedure similar to P-aptmds, except that APTMDS was substituted by APPDMS. The product was obtained in 71% yield.

1,3-Bis(3-(8-allyl-2H-benzo[e][1,3]oxazin-3(4H)-yl)propyl)-1,1,3,3-tetramethyldisiloxane (oAP-APTMDS). *o*AP-aptmds was synthesized by a procedure similar to P-aptmds, except that phenol (11.5 mL) was substituted by *o*-allylphenol (16 mL). The product was obtained in 78% yield.

α,ω-Bis(3-(8-allyl-2H-benzo[e][1,3]oxazin-3(4H)-yl)propyl)polydimethylsiloxane (oAP-APPDMS). *o*AP-appdms was synthesized by a procedure similar to *o*AP-aptmds, except that APTMDS was substituted by APPDMS. The product was obtained in 71% yield.

Preparation of Polybenzoxazines

First, a siloxane-containing benzoxazine was poured into a steel mold, and the mold was put into a vacuum oven. Then, for P-aptmds, the vacuum oven was step-heated to 120 and 150 °C, and held at each temperature for 2 h, and then held at 180 °C for 6 h; and for P-appdms, *o*AP-aptmds, and *o*AP-appdms, the vacuum oven was step-heated to 120 and 150 °C, and held at each temperature for 2 h, and then held at 200 °C for 6 h. The resultant polybenzoxazines from P-aptmds, P-appdms, *o*AP-aptmds, and *o*AP-appdms are designated as poly(P-aptmds), poly(P-appdms), poly (*o*AP-aptmds), and poly(*o*AP-appdms), respectively.

Measurements

^{1}H, ^{13}C, and ^{29}Si nuclear magnetic resonance (NMR) spectra were recorded using a Bruker Avance III 600 NMR spectrometer. Deuterated chloroform ($CDCl_3$) was used as the solvent. Chemical shifts of ^{1}H and ^{13}C are given in parts per million from internal tetramethylsilane (TMS) and the shifts for ^{29}Si from external TMS. Solid-state NMR experiments were performed at room temperature (25 °C) on a Bruker Avance III 400 NMR spectrometer operating at a ^{13}C resonance frequency of 100.568 MHz. The samples were analyzed under crosspolarization/magic-angle spinning (CP/MAS) conditions using 4-mm zirconia rotors at a spinning frequency of 5 kHz. A 90° pulse width of 4 ms was employed, and the CP Hartmann-Hahn contact time was set at 3.0 ms. The chemical shifts of ^{13}C spectra were externally referenced to the carbon signal of solid adamantane (38.48 ppm relative to TMS).

The Fourier transform infrared (FTIR) spectra were obtained with a Nicolet 380 FTIR spectrometer at a resolution of 4 cm^{-1}. A siloxane-containing benzoxazine monomer or telechelic benzoxazine oligomer sample was dissolved in chloroform, and the solution was coated on a KBr disk to form a thin uniform film. When the solvent was completely evaporated at 50 °C in a vacuum oven, the disk was scanned by the FTIR spectrometer. Thereafter, the disk was heated isothermally in a static air oven. During the polymerization reaction, the disk to be scanned was removed periodically.

The dynamic polymerization reactions for the siloxane-containing benzoxazine monomer and telechelic benzoxazine oligomers were monitored by a PerkinElmer Diamond differential scanning calorimeter operating in nitrogen, and the samples were scanned at a heating rate of 10 °C/min.

A Perkin-Elmer DMA-8000 dynamic mechanical analyzer was used to determine the dynamic storage modulus (E') and loss factor (tan δ) using single cantilever bending mode. Measurements were performed on rectangular specimens with dimensions of approximately 10.0 mm × 6.0 mm × 2.0 mm by heating from −50 to 250 °C, with a heating rate of 2 °C/min and a frequency of 1 Hz.

The shape memory properties of poly(*o*AP-aptmds) were demonstrated by a series of photos recorded in the shape recovery process for a specimen deformed under bending mode. A rectangular molded sheet specimen with dimensions of 100.0 mm × 6.0 mm × 2.0 mm was isothermally heated at approximately 60 °C for several minutes, coiled into a spiral circling a rod with a diameter of approximately 10 mm, and plunged into ice water under constrained condition to fix the temporary shape. Then, the spiral was isothermally heated at approximately 30 °C to recover the permanent shape.

The bending shape recovery behavior of poly(*o*AP-aptmds) was quantitatively investigated under bending deformation mode. In bending test (fold-deploy test), a rectangular molded sheet specimen with dimensions of approximately 30 mm × 6.0 mm × 2.0 mm was isothermally heated at approximately 60 °C for several minutes, and then the sheet specimen was bent into a U-shape circling a rod with a diameter of 5 mm and plunged into ice water to fix the temporary shape (corresponding angle-θ_{max}) under a constant external force. Subsequently, the specimen was unloaded, and one side of the U-shape sheet was fixed on a device which can measure the deflection angle of the free side of the U-shape sheet. Thereafter, the device was immediately placed into an oven at a desired temperature, and the shape recovery process was monitored. The folded angle (θ_{max}, a fold angle of 180° was made on all specimens), fixed angle (θ_{fix}), and residual angle (θ_i) were measured and the shape fixity ratio (R_f) and shape recovery ratio (R_r) were calculated by the following equations.

$$R_f = \frac{\theta_{fix}}{\theta_{max}} \times 100\% \quad (1)$$

$$R_r = \frac{\theta_{max} - \theta_i}{\theta_{max}} \times 100\% \quad (2)$$

The tension shape memory behaviors of poly(P-aptmds), poly(*o*AP-aptmds), poly(P-appdms) were characterized by a TA Instruments Q800 dynamic mechanical analyzer using the tensile film clamp in controlled force mode. A rectangular molded sheet specimen with dimensions of approximately 10.0 mm × 5.0 mm × 1.0 mm was heated from room temperature to $T_g + 10$ °C at 5 °C/min, and held at this temperature for 3 min. Then, the specimen was uniaxially elongated isothermally by ramping force to a designed strain (ε_m) at a rate of 0.5 N/min. Thereafter, the specimen was cooled under constant load to $T_g - 40$ °C at a rate of 5 °C/min to fix the temporary shape. The force on the specimen was unloaded at a rate of 0.5 N/min to ensure shape fixing. Upon unloading, part of the strain ($\varepsilon_m - \varepsilon_u$) was instantaneously recovered, leaving an unloading strain (ε_u). Finally, the specimen was reheated at a rate of 3 °C/min to $T_g + 10$ °C and held at that temperature for a certain time to recover any residual strain. The recovery process left a permanent strain (ε_p). The shape fixity ratio (R_f) and shape recovery ratio (R_r) were calculated using the following equations:

$$R_f = \frac{\varepsilon_u}{\varepsilon_m} \times 100\% \quad (3)$$

$$R_r = \frac{\varepsilon_m - \varepsilon_p}{\varepsilon_m} \times 100\% \quad (4)$$

where ε_m, ε_u, and ε_p denote the strain after the stretching step (before unloading the specimen), the strain in the fixed temporary shape, the strain after recovery, respectively.

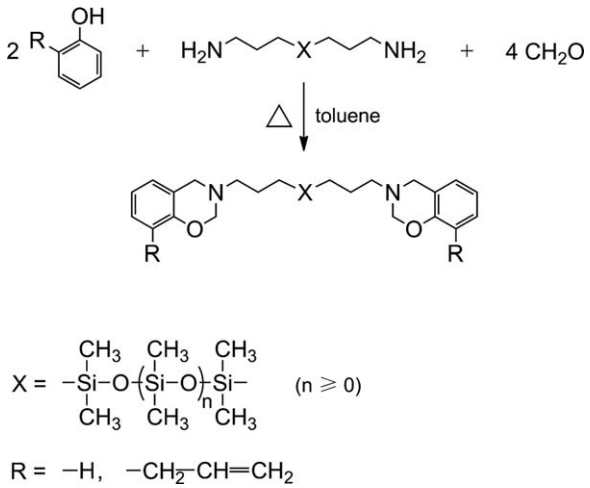

Scheme 1. Synthesis of P-aptmds, P-appdms, oAP-aptmds, and oAP-appdms.

RESULTS AND DISCUSSION

Synthesis of Siloxane-Containing Benzoxazine Monomers and Telechelic Benzoxazine Oligomers

Four siloxane-containing benzoxazine monomers and telechelic benzoxazine oligomers were synthesized from APTMDS, APPDMS, phenol, *o*-allylphenol, and formaldehyde,[32] and the synthesis mechanism is shown in Scheme 1. The chemical structures of the siloxane-containing benzoxazine monomers and telechelic benzoxazine oligomers were confirmed by ^{1}H, ^{13}C, ^{29}Si NMR and FTIR spectra.

The ^{1}H, ^{13}C, ^{29}Si NMR spectra of P-aptmds, P-appdms, oAP-aptmds, and oAP-appdms are presented in Supporting Information Figures S1 and S2. In the ^{1}H NMR spectra, the resonances at 3.98–4.00 and 4.87–4.89 ppm correspond to the methylene protons of Ar—CH_2—N and O—CH_2—N of the oxazine ring,[22] respectively. The chemical shifts (ppm) at 0.06–0.09 correspond to the protons in the methyl groups of tetramethyldisiloxane (TMDS) and polydimethylsiloxane (PDMS) units, and 0.52–0.58, 1.56–1.63, and 2.70–2.76 are assigned to the protons of the aminopropyl group,[22] whereas the chemical shifts (ppm) at 3.33–3.36, 5.02–5.08, and 5.96–6.04 correspond to the aliphatic protons in the allyl group.[32,33] The peaks at 6.77–7.13 ppm are assigned to the aromatic protons.

In the ^{13}C NMR spectra, the resonances at 54.51–54.66 and 82.46–82.53 ppm correspond to the methylene carbons of Ar—CH_2—N and O—CH_2—N of the oxazine ring,[22] respectively. The chemical shifts (ppm) at 0.08–0.97 correspond to the carbons in the methyl groups of TMDS and PDMS units, and 15.49–15.70, 21.87–22.06, and 50.19–50.37 are assigned to the carbons of the aminopropyl group,[34] whereas the chemical shifts (ppm) at 33.48–33.57, 115.15–115.22, and 136.68–136.78 correspond to the aliphatic carbons in the allyl group.[32,33] The detail assignments of other chemical shifts can be seen in Supporting Information Figures S1 and S2.

In the ^{29}Si NMR spectra, the resonances at 7.61–7.63 ppm correspond to the silicon atoms in the TMDS backbone, whereas the resonance at 7.47–7.48 ppm corresponds to the silicon on

the end of the PDMS units, and the resonances at −22.06 to −21.41 ppm correspond to the different silicon atoms in the PDMS backbone.[34]

The FTIR spectra of P-aptmds, P-appdms, oAP-aptmds, and oAP-appdms are presented in Supporting Information Figure S3. In the FTIR spectra, the asymmetric stretching vibrations of C—O—C of the oxazine ring are observed at 1223–1226 cm^{-1}.[35] The absorption at 925 cm^{-1} is the characteristic mode of the benzene ring with an oxazine ring attached. The olefinic C═C stretching vibration at 1638 cm^{-1} and the olefinic C—H out-of-plane bending vibration at 994 cm^{-1} belong to the characteristic absorptions of the allyl group, and the olefinic ═C—H stretching vibration of the allyl group appear at 3075 cm^{-1}.[32] The peaks at 3040–3045 cm^{-1} are the ═C—H stretching vibrations of the aromatic ring. The C—H asymmetric stretching vibrations of CH_3 and CH_2 are at 2952–2961 and 2926–2930 cm^{-1}, respectively, whereas and the C—H stretching vibrations of CH are at 2892–2896 cm^{-1}, and the C—H symmetric stretching vibrations of CH_3 and CH_2 are at 2896–2903 and 2856–2863 cm^{-1}, respectively. The absorption peaks at bands of 1456–1464 and 1302–1341 cm^{-1} are due to CH_2 bending and wagging vibrations, respectively, whereas the CH_3 bending vibration is observed at 1372 cm^{-1}. The bands at 1253–1260 cm^{-1} are due to the Si—CH_3 bending deformation, and the absorption peaks at 1055–1091 cm^{-1} are assigned to the asymmetric stretching vibrations of Si—O—Si.[36] while the bands at 796–800 cm^{-1} are owing to the stretching vibrations of Si—C.[36] The absorptions at 1608, 1594, 1584, and 1488 cm^{-1} are associated with the C═C stretching vibrations of the aromatic ring, and the peak at 1109 cm^{-1} is ascribed to the C—H in-plane bending vibration of the aromatic ring, whereas the bands at 838, 753, 748, and 706 cm^{-1} are attributed to the C—H out-of-plane bending vibrations of the aromatic ring.

Polymerization Behavior

Figure 1 presents the dynamic DSC curves of P-aptmds, P-appdms, *o*AP-aptmds, and *o*AP-appdms. Each DSC curve shows an exothermic peak with an onset polymerization temperature of 166, 208, 160, and 170 °C for P-aptmds, P-appdms, *o*AP-aptmds, and *o*AP-appdms, respectively, and a peak temperature centered at 219, 237, 215, and 234 °C, respectively. Obviously, the onset polymerization temperatures of the two benzoxazines based on APTMDS are lower than those of their counterparts (telechelic benzoxazine oligomers) based on APPDMS, indicating that the reactivity of the benzoxazines with a shorter siloxane segment is higher than that of their counterparts with a longer siloxane segment. Moreover, it also can be observed that the DSC curves exhibit a relatively weak exothermic peak for P-aptmds and *o*AP-aptmds, but a strong exothermic peak for P-appdms and *o*AP-appdms, implying that the polymerization of the benzoxazines based on APTMDS proceeds slowly and the highest reaction rate is lower than those of their counterparts based on APPDMS. Therefore, the length of the siloxane segment has significant influence on the polymerization reaction of the benzoxazines. Owing to the two oxazine rings are bridged by an alkyl-siloxane segment, the effectiveness of the crosslinks formed by the telechelic benzoxazine oligomers based on APPDMS in restricting the reactivity is less than that

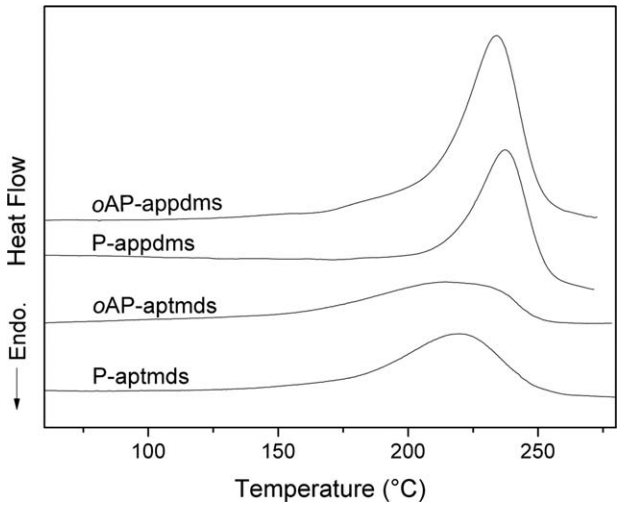

Figure 1. The non-isothermal DSC curves for P-aptmds, P-appdms, oAP-aptmds, and oAP-appdms.

of the benzoxazine monomers based on APTMDS, indicating that an increase in the spacer length between the oxazine rings increases the ring-opening polymerization rate. Therefore, the reactivity and reaction rate in the polymerization of the benzoxazine monomers and telechelic benzoxazine oligomers based on aminopropyl terminated siloxanes are defined by the length of the siloxane segment.

Structure Changes in Polymerization

Supporting Information Figure S4 presents the FTIR spectra of P-aptmds, P-appdms, oAP-aptmds, oAP-appdms, and their polymerized products obtained at different temperatures for various times, respectively. As can be seen, the characteristic changes in the polymerization are the decrease of the intensities of the peaks related to the oxazine ring, such as the peaks of the asymmetric stretching vibration of C—O—C of the oxazine ring at 1210–1226 cm^{-1} and the characteristic mode of the benzene ring with an oxazine ring attached at 925–929 cm^{-1}. Meanwhile, the intensities of some peaks related to the aromatic ring decrease obviously, such as the peaks of at 1584, 1488, 753, 706, and 587 cm^{-1} for the benzoxazine monomers and telechelic benzoxazine oligomers based on phenol. Consequently, the phenolic OH stretching vibration appears in the region of 3300–3500 cm^{-1} and increases with rising reaction time. Moreover, a new peak appears at 1633–1638 cm^{-1} and increases obviously with rising time, which is attributed to the formation of the C═N bond of Schiff base.[37–39] At the same time, the intensity of the peak at 1680 cm^{-1} also increases, which is due to the C═O stretching of Ar—CO—NH—CH_3 structure formed in the oxazine ring-opening.[40] Furthermore, the decrease in the intensity of the peaks at 3075 cm^{-1} [Supporting Information Figure S4(c,d)] and 994 cm^{-1} [Supporting Information Figure S4(c)] confirm the addition reaction of the olefinic C═C bond of the allyl group.

Based on the mechanism of ring-opening polymerization of benzoxazines,[32,41–45] the structure changes from benzoxazine monomers and telechelic benzoxazine oligomers to the resultant polybenzoxazines can be described by Scheme 2.

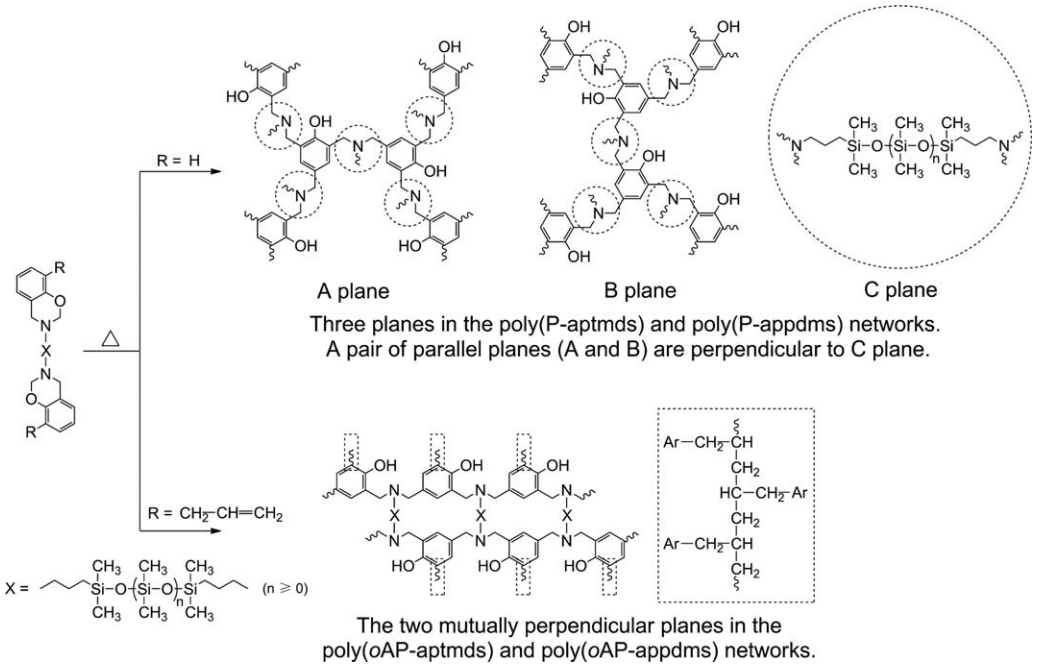

Scheme 2. Structural changes from benzoxazine monomers and telechelic benzoxazine oligomers to polybenzoxazines.

In addition, to demonstrate the structure changes from monomers to polymers, Supporting Information Figures S5 and S6 present the solid-state ^{13}C CP/MAS NMR spectra of P-aptmds, P-appdms, *o*AP-aptmds, *o*AP-appdms, and their corresponding polybenzoxazines, respectively. The assignments of the peaks in the ^{13}C CP/MAS NMR spectra of P-aptmds, P-appdms, *o*AP-aptmds, and *o*AP-appdms coincide with those of the deuterium chloroform solution-state ^{13}C NMR spectra in Supporting Information Figures S1 and S2, respectively. Comparing the variation in chemical shift of the characteristic carbons from monomer to polymer, it can be noticed that the resonance peaks of the methylene carbons of the oxazine ring disappear and a new resonance peak appears corresponding to the chemical shift of the methylene carbons of the Mannich bridge structure. Meanwhile, a resonance peak at 33.26–33.32 ppm (labeled "*" in Supporting Information Figure S5) appeared in the ^{13}C CP/MAS NMR spectra of both polybenzoxazines based on phenol, which may be due to the resonance of a possible terminal methyl carbon in Ar—CO—NH—CH_3 structure formed by a methylene of the oxazine ring.[40] However, the changes in chemical shift of the olefinic unsaturated carbons of the allyl groups of *o*AP-aptmds and *o*AP-appdms are difficult to discern due to the overlap of the resonance peaks of the three saturated carbons from the allyl group (Supporting Information Figure S6). Obviously, the resonance peaks in Supporting Information Figure S6 show that unreacted olefinic unsaturated carbons remain in *o*-allylphenol-based polybenzoxazines. Moreover, the chemical shifts of the aromatic and saturated aliphatic carbons remain unchanged, but most of the resonance peaks of these carbons become highly overlapped.

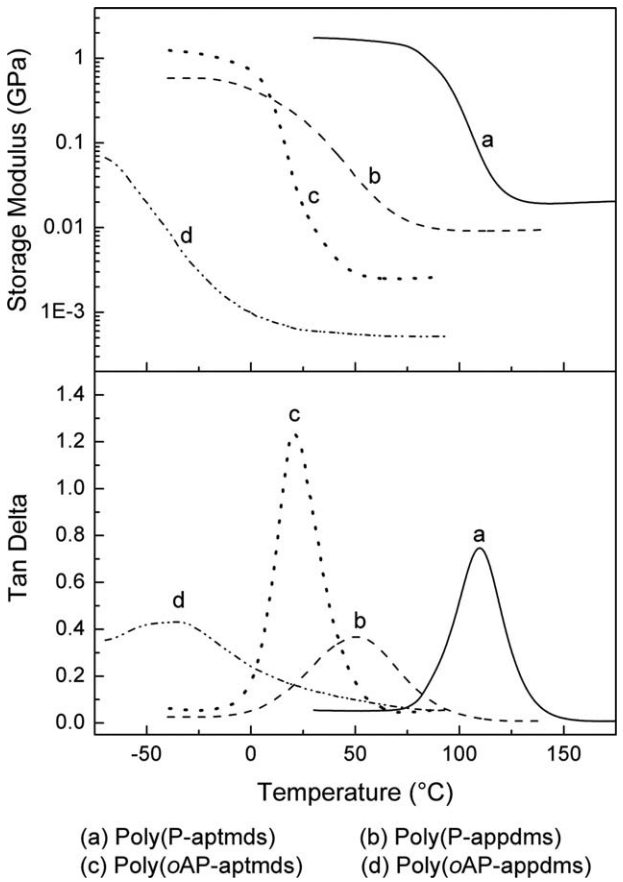

Figure 2. The curves of E' and tan δ as a function of temperature for poly (P-aptmds), poly(P-appdms), poly(oAP-aptmds), and poly(oAP-appdms).

Dynamic Mechanical Properties

Figure 2 presents the curves of the storage modulus (E') and loss factor (tan δ) versus temperature for poly(P-aptmds), poly (P-appdms), poly(oAP-aptmds), and poly(oAP-appdms). As can be seen, the influence of the phenol structure is stronger than that of the siloxane segment length on the E' and tan δ of the

Table I. Analysis of the DMA Curves of Polybenzoxazines

Polybenzoxazine	T_g (°C)	Height of tan δ peak	Width of tan δ peak (half ht.) (°C)	ρ ($\times 10^{-3}$) (mol cm^{-3})
Poly(P-aptmds)	110	0.75	27	1.90
Poly(P-appdms)	50	0.37	53	0.99
Poly(oAP-aptmds)	20	1.24	24	0.30
Poly(oAP-appdms)	−35	0.43	—	0.08

polybenzoxazines. In the glassy state, the E's of the polybenzoxazines decrease in the following order: poly(P-aptmds) > poly(*o*AP-aptmds) > poly(P-appdms) > poly(*o*AP-appdms), indicating that the stiffness of the polybenzoxazines based on APTMDS are higher than those of the APPDMS counterparts in the glassy state. With increasing temperature, the E's of the polybenzoxazines based on APTMDS decrease more quickly than those of the APPDMS counterparts, resulting in a narrower transition temperature range from glassy state to rubbery state.

According to the statistical theory of rubber elasticity,[46] the rubbery plateau is associated with the crosslinking density of materials, and the crosslinking density for lightly crosslinked materials can be estimated from the rubbery plateau modulus using following equation[47,48]:

$$\rho = E'_e / 3\phi RT \quad (5)$$

where E'_e is the equilibrium elastic modulus in the rubbery plateau, φ is a front factor, which is unity for ideal rubbers, R is the gas constant, T is the absolute temperature, and ρ is the crosslinking density, which is the mole number of network chains per unit volume of the polymers.

Table I lists the calculated crosslinking density results, peak heights, peak widths at half-height, and the T_g values determined from the tan δ peak temperatures for the four polybenzoxazines. Though the polymerization of allyl groups can provide additional crosslinking points, the crosslinking density of poly(*o*AP-aptmds) is much lower than those of the phenolic counterparts due to the blocking effect of the *ortho*-position on the polymerization, implying that the chain flexibility in poly(*o*AP-aptmds) is higher than in the phenolic counterparts. In theory, increasing length of the siloxane segment leads to decreasing crosslinking density of the network, due to the increase of the average molecule weight between crosslinking points. At the same time, on increasing length of the siloxane segment, the crosslinking points are far more linked together with higher flexible segment mobility. In general, the crosslinking density of networks is highly influential on T_g, and a low crosslinking density would result in a low T_g value. In addition, the height of the tan δ peaks of poly(*o*AP-aptmds) is much higher than other three polybenzoxazines, indicating that the mobility of the molecular chains in poly(*o*AP-aptmds) is the highest. But, the peak width at half-height of the tan δ peaks of poly(P-aptmds) and poly(P-appdms) is broader than that of poly(*o*AP-aptmds), implying that poly(P-aptmds) and poly(P-appdms) have more number of kinetic units adequately to move than poly(*o*AP-aptmds), which results in a broader distribution of structures for poly(P-aptmds) and poly(P-appdms) over poly(*o*AP-aptmds).

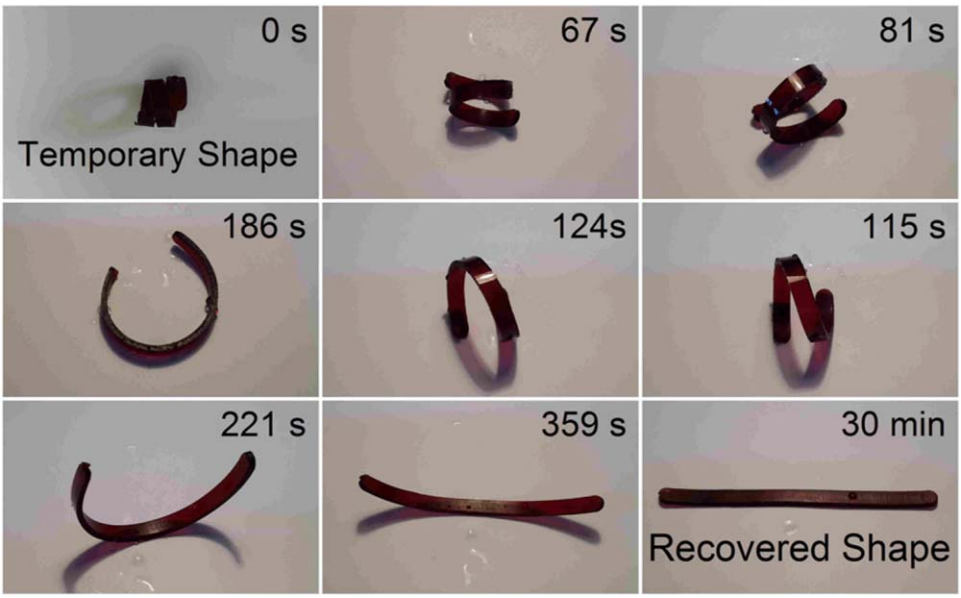

Figure 3. Photographs of a specimen of poly(oAP-aptmds) showing the shape recovery process from a temporary shape to the recovered shape at 30 °C. [Color figure can be viewed in the online issue, which is available at wileyonlinelibrary.com.]

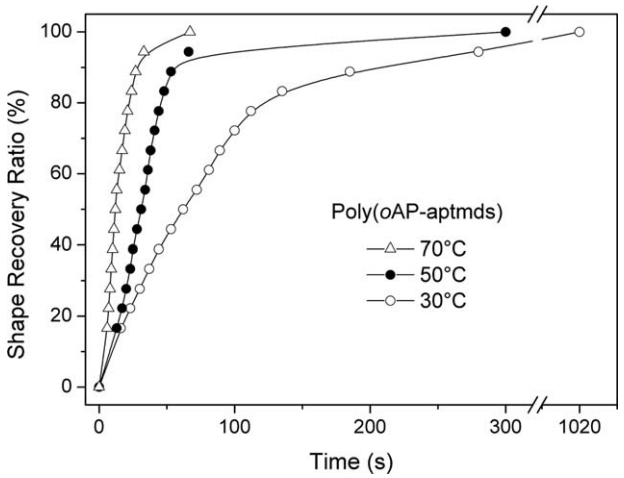

Figure 4. The plots of the shape recovery ratio versus time for poly(oAP-aptmds) at different temperatures.

Shape-Memory Properties

In the four polybenzoxazines based on aminopropyl-terminated siloxanes, poly(P-aptmds), poly(*o*AP-aptmds), and poly(P-appdms) exhibit a thermally induced one-way dual-shape SME, but the shape memory behavior of poly(*o*AP-appdms) was not confirmed due to the poor shape fixity. To demonstrate the SME qualitatively, Figure 3 presents a series of photographs taken in the shape recovery process for a specimen of poly(*o*AP-aptmds) in bending deformation mode. The photographs show a one-way shape recovery behavior of a temporary spiral specimen of poly(*o*AP-aptmds) deformed from a rectangular molded sheet, and the specimen in the shape memory test shows excellent shape fixity and high shape recovery.

In addition, the bending shape memory behavior of poly(*o*AP-aptmds) was quantitatively tested under bending mode. In the fold-deploy test, a rectangular molded sheet specimen was bent into a "U" shape with a fold angle of 180° at a temperature above T_g. Subsequently, the U-shape sheet was cooled to T_g – 20 °C under a constant stress. The R_fs for all specimens were all 100%. Then the U-shape sheet was heated isothermally to recover the original shape. Figure 4 presents the results of poly(*o*AP-aptmds) from the fold-deploy test. With increasing temperature, the time decreased to reach a certain R_r. The same fold angle (180°) was recovered by 100% in 1020, 300, and 67 s at 30, 50, and 70 °C for the specimens of poly(*o*AP-aptmds), respectively, which indicates that the fold angle can be fully recovered and the recovery time decreases with rising temperature.

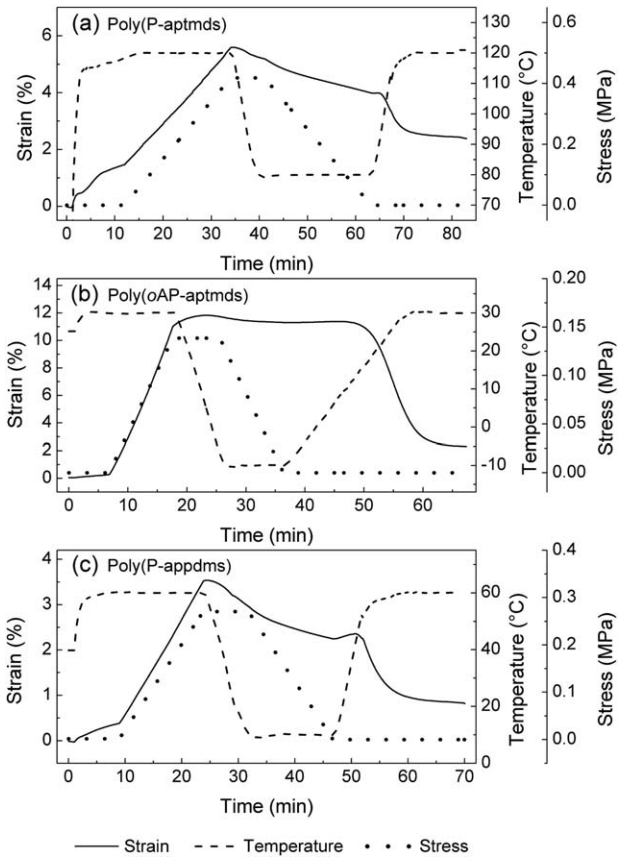

Figure 5. The evolution of stress, strain, and temperature with time for poly (P-aptmds), poly(*o*AP-aptmds), and poly(P-appdms) in tensile stress–strain test.

Moreover, to characterize the tension shape memory behavior quantitatively, a tensile stress–strain test was made on specimens of poly(P-aptmds), poly(*o*AP-aptmds), and poly(P-appdms), respectively. In the tensile stress–strain test, a rectangular molded sheet specimen was isothermally stretched to a certain elongation at T_g + 10 °C, then cooled to T_g – 40 °C for poly(P-aptmds) and poly(P-appdms) and to T_g – 30 °C for poly(*o*AP-aptmds) to fix in a temporary shape, and finally heated to

Table II. Shape Memory Parameters for Polybenzoxazines in Bending and Tensile Stress–Strain Tests

Deformation mode	Polybenzoxazine	Fixing temperature (°C)	R_f (%)	Recovering temperature (°C)	R_r (%)
Spiral-shape—bending	Poly(oAP-aptmds)	0	100	30	100
U-shape—bending	Poly(oAP-aptmds)	0	100	30	100
		0	100	50	100
		0	100	70	100
Tensile—stress-strain	Poly(P-aptmds)	70	71.4	120	57.1
	Poly(oAP-aptmds)	−10	96.5	30	79.6
	Poly(P-appdms)	10	62.9	60	77.1

$T_g + 10\,^{\circ}C$ to recover the permanent shape. Figure 5 shows the evolution of stress, strain, and temperature with time during the shape memory test for poly(P-aptmds), poly(*o*AP-aptmds), and poly(P-appdms), respectively. As can be seen, the maximum strains and the final residual strains were 5.6 and 2.4% for poly(P-aptmds), 11.8 and 2.3% for poly(oAP-aptmds), and 3.5 and 0.8% for poly(P-appdms), respectively. Calculated with the data from the strain curves, the R_f and R_r are summarized in Table II. Obviously, both the R_f and R_r of poly(*o*AP-aptmds) are, respectively, higher than those of poly(P-aptmds) and poly(P-appdms), which is due to the structure difference between the polybenzoxazine networks. The low crosslinking density and the flexible allyl groups in the poly(*o*AP-aptmds) network contribute to the higher R_f and R_r of poly(*o*AP-aptmds) over poly(P-aptmds) and poly (P-appdms). In addition, the R_f of poly(P-aptmds) is higher than that of poly(P-appdms), whereas the R_r of poly(P-aptmds) is lower than that of poly(P-appdms), due to the difference in crosslinking density resulted from different length of siloxane segment between poly(P-aptmds) and poly(P-appdms).

Comparing to the results obtained in the bending test (fold-deploy test) (Some results were summarized in Table II), the value of R_r in the tensile stress–strain test for poly(*o*AP-aptmds) is low, which may be due to the occurrence of a permanent plastic deformation in the stretching process or relaxation during the subsequent fixing and recovering processes. Thus, the SME of the specimens of poly(*o*AP-aptmds) are affected by the programmed testing conditions, such as the deformation mode, deformation temperature, rates of loading and unloading, rates of cooling and reheating, recovering mode. Similar phenomenon was observed in the previous reports for other polybenzoxazines.[17,18] The effect of the programmed testing conditions on the SME is associated with the crosslinking density of the networks and the flexibility of the switching segments of polybenzoxazines.

The shape memory performance of the polybenzoxazines based on aminopropyl-terminated siloxanes depends on their network structures. In the polybenzoxazine SMP network, the chemical or physical crosslinking points serve as the fixity phase to memorize the permanent shape, and the flexible alkyl-siloxane units act as switch segments to fix the temporary shape. The alkyl-siloxane units are effective switching segments in which the T_g serves as a transition temperature of the networks of the polybenzoxazines.

CONCLUSIONS

Four benzoxazine monomers and telechelic benzoxazine oligomers based on aminopropyl-terminated siloxanes were synthesized. The polymerization of the benzoxazine monomers and telechelic benzoxazine oligomers, the dynamic mechanical and shape memory properties of the resultant polybenzoxazines are strongly affected by the phenol structure and the length of siloxane segment. The glass transition temperatures of the polybenzoxazines based on APTMDS are higher than those of their counterparts based on APPDMS. These polybenzoxazines exhibit one-way dual-shape memory effect in response to changes in temperature, and the shape memory performance of the polybenzoxazine based on *o*-allylphenol and 1,3-bis(3-aminopropyl)−1,1,3,3-tetramethyldisiloxane is higher than those of phenol-based polybenzoxazines.

ACKNOWLEDGMENTS

This work was financially supported by the Natural Science Foundation of Hebei Province (B2013201107).

REFERENCES

1. Lendlein, A.; Kelch, S. *Angew. Chem., Int. Ed.* **2002**, *41*, 2034.
2. Xie, T. *Polymer* **2001**, *52*, 4985.
3. Hager, M. D.; Bode, S.; Weber, C.; Schubert, U. S. *Prog. Polym. Sci.* **2015**, *49-50*, 3.
4. Hu, J. L.; Zhu, Y.; Huang, H. H.; Lu, J. *Prog. Polym. Sci.* **2012**, *37*, 1720.
5. Zhao, Q.; Qi, H. J.; Xie, T. *Prog. Polym. Sci.* **2015**, *49–50*, 79.
6. Julich-Gruner, K. K.; Löwenberg, C.; Neffe, A. T.; Behl, M.; Lendlein, A. *Macromol. Chem. Phys.* **2013**, *214*, 527.
7. Behl, M.; Kratz, K.; Zotzmann, J.; Nöchel, U.; Lendlein, A. *Adv. Mater.* **2013**, *25*, 4466.
8. Burke, K. A.; Rousseau, I. A.; Mather, P. T. *Polymer* **2014**, *55*, 5897.
9. Bao, M.; Lou, X. X.; Zhou, Q. H.; Dong, W.; Yuan, H. H.; Zhang, Y. Z. *ACS Appl. Mater. Interfaces* **2014**, *6*, 2611.
10. Song, J. J.; Chang, H. H.; Naguib, H. E. *Polymer* **2015**, *56*, 82.
11. Ahn, S. K.; Deshmukh, P.; Kasi, R. M. *Macromolecules* **2010**, *43*, 7330.
12. Liu, Y. J.; Du, H. Y.; Liu, L. W.; Leng, J. S. *Smart Mater. Struct.* **2014**, *23*, 023001.
13. Erden, N.; Jana, S. C. *Macromol. Chem. Phys.* **2013**, *214*, 1225.
14. Gu, S. L.; Jana, S. *Polymers* **2014**, *6*, 1008.
15. Rimdusit, S.; Lohwerathama, M.; Hemvichian, K.; Kasemsiri, P.; Dueramae, I. *Smart Mater. Struct.* **2013**, *22*, 075033.
16. Tanpitaksi, T.; Jubsilp, C.; Rimdusit, S. *Expr. Polym. Lett.* **2015**, *9*, 824.
17. Liu, Y. F.; Li, Y. H.; Zhang, C. H.; Wang, R. R.; Run, M. T.; Song, H. Z. *J. Polym. Sci. Part B: Polym. Phys.* **2016**, *54*, 1255.
18. Liu, Y. F.; Huang, J. B.; Su, X. H.; Han, M.; Li, H.; Run, M. T.; Song, H. Z.; Wu, Y. G. *React. Funct. Polym.* **2016**, *102*, 62.
19. Liu, Y. L.; Hsu, C. W.; Chou, C. I. *J. Polym. Sci. Part A: Polym. Chem.* **2007**, *45*, 1007.
20. Hsieh, C. Y.; Su, W. C.; Wu, C. S.; Lin, L. K.; Hsu, K. Y.; Liu, Y. L. *Polymer* **2013**, *54*, 2945.
21. Wang, L.; Zheng, S. X. *Polymer* **2010**, *51*, 1124.
22. Takeichi, T.; Kano, T.; Agag, T.; Kawauchi, T.; Furukawa, N. *J. Polym. Sci. Part A: Polym. Chem.* **2010**, *48*, 5945.
23. Li, W. Z.; Chu, J.; Heng, L.; Wei, T.; Gu, J. J.; Xi, K.; Jia, X. D. *Polymer* **2013**, *54*, 4909.
24. Chen, K. C.; Li, H. T.; Chen, W. B.; Liao, C. H.; Sun, K. W.; Chang, F. C. *Polym. Int.* **2011**, *60*, 436.

25. Chen, K. C.; Li, H. T.; Huang, S. C.; Chen, W. B.; Sun, K. W.; Chang, F. C. *Polym. Int.* **2011**, *60*, 1089.
26. Zhu, C. L.; Wei, Y. Z.; Zhang, J.; Geng, P. F.; Lu, Z. J. *J. Appl. Polym. Sci.* **2014**, *131*, DOI: 10.1002/app40960.
27. Kiskan, B.; Aydogan, B.; Yagci, Y. *J. Polym. Sci. Part A: Polym. Chem.* **2009**, *47*, 804.
28. Aydogan, B.; Sureka, D.; Kiskan, B.; Yagci, Y. *J. Polym. Sci. Part a: Polym. Chem.* **2010**, *48*, 5156.
29. kumar, R. S.; Padmanathan, N.; Alagar, M. *New J. Chem.* **2015**, *39*, 3995.
30. Nakamura, M.; Ishida, H. *Polymer* **2009**, *50*, 2688.
31. Wang, H.; Wang, J.; Feng, T. T.; Ramdani, N.; Li, Y; Xu, X. D.; Liu, W. B. *J. Therm. Anal. Calorim.* **2015**, *119*, 1913.
32. Liu, Y. F.; Liao, C. Y.; Hao, Z. Z.; Luo, X. X.; Jing, S. S.; Run, M. T. *React. Funct. Polym.* **2014**, *75*, 9.
33. Liu, Y. F.; Zhang, J.; Li, Z. Y.; Luo, X. X.; Jing, S. S.; Run, M. T. *Polymer* **2014**, *55*, 1688.
34. Pozos vázquez, C.; Tayouo, R.; Joly-Duhamel, C.; Boutevin, B. *J. Polym. Sci. Part A: Polym. Chem.* **2010**, *48*, 2123.
35. Dunkers, J.; Ishida, H. *Spectrochim. Acta* **1995**, *51A*, 1061.
36. Maya, E. M.; Snow, A. W.; Buckley, L. J. *Macromolecules* **2002**, *35*, 460.
37. Kim, H. J.; Brunovska, Z.; Ishida, H. *Polymer* **1999**, *40*, 1815.
38. Allen, D. J.; Ishida, H. *Polymer* **2007**, *48*, 6763.
39. Shen, S. B.; Ishida, H. *J. Appl. Polym. Sci.* **1996**, *61*, 1595.
40. Zhang, X. Q.; Potter, A. C.; Solomon, D. H. *Polymer* **1998**, *39*, 399.
41. Takeichi, T.; Nakamura, K.; Agag, T.; Muto, H. *Des. Monomers Polym.* **2004**, *7*, 727.
42. Allen, D. J.; Ishida, H. *Polymer* **2009**, *50*, 613.
43. Liu, C.; Shen, D.; Sebastián, R. M.; Marquet, J.; Schönfeld, R. *Macromolecules* **2011**, *44*, 4616.
44. Wang, J.; He, X. Y.; Liu, J. T.; Liu, W. B.; Yang, L. *Macromol. Chem. Phys.* **2013**, *214*, 617.
45. Liu, C.; Shen, D.; Sebastián, R. M.; Marquet, J.; Schönfeld, R. *Polymer* **2013**, *54*, 2873.
46. Treloar, L. R. G. The Physics of Rubber Elasticity; Oxford University Press: London, **1949**; p 66.
47. Allen, D. J.; Ishida, H. *J. Appl. Polym. Sci.* **2006**, *101*, 2798.
48. Velez-Herrera, P.; Doyama, K.; Abe, H.; Ishida, H. *Macromolecules* **2008**, *41*, 9704.